

Modeling secondary organic aerosol formation from isoprene oxidation under dry and humid conditions

F. Couvidat and C. Seigneur

CEREA, Joint Laboratory École des Ponts ParisTech/EDF R&D, Université Paris-Est, 77455 Marne la Vallée, France

Received: 22 July 2010 – Published in Atmos. Chem. Phys. Discuss.: 30 August 2010

Revised: 1 December 2010 – Accepted: 14 January 2011 – Published: 31 January 2011

Abstract. A new model for the formation of secondary organic aerosol (SOA) from isoprene was developed. This model uses surrogate molecular species (hydroxy-hydroperoxides, tetrols, methylglyceric acid, organic nitrates) to represent SOA formation. The development of this model used available experimental data on yields and molecular composition of SOA from isoprene and methacrolein oxidation. This model reproduces the amount of particles measured in smog chambers under both low-NO_x and high-NO_x conditions. Under low-NO_x conditions, the model reproduces the transitional formation of hydroxy-hydroperoxides particles, which are photolyzed and lead to SOA mass decrease after reaching a maximum. Under high-NO_x conditions, particles are assumed to be formed mostly from the photo-oxidation of a PAN-type molecule derived from methacrolein (MPAN). This model successfully reproduces the complex NO_x-dependence of isoprene oxidation and suggests a possible yield increase under some high-NO_x conditions. Experimental data correspond to dry conditions (RH < 10%). However, particles formed from isoprene are expected to be highly hydrophilic, and isoprene oxidation products would likely partition between an aqueous phase and the gas phase at high humidity in the atmosphere. The model was extended to take into account the hydrophilic properties of SOA, which are relevant under atmospheric conditions, and investigate the effect of particulate liquid water on SOA formation. An important increase in SOA mass was estimated for humid conditions due to the hydrophilic properties. Experiments under high relative humidity conditions should be conducted to confirm the results of this study, which have implications for SOA modeling.

1 Introduction

Atmospheric fine particles are known to have effects on health, atmospheric visibility, materials and climate. Among those particles, particulate organic matter (POM) represents a large fraction of the particulate mass, typically between 20 and 60% (Kanakidou et al., 2005; Yu et al., 2007; Zhang et al., 2007a). Those particles are either primary (directly emitted as particles) or secondary (particles formed by chemical reactions in the atmosphere). In the latter case, secondary organic aerosols (SOA) are formed by the gas-to-particle partitioning of the oxidation products of volatile organic compounds (VOCs). VOCs are emitted by both anthropogenic and biogenic sources. However, SOA formation is poorly understood due to the numerous and complex chemical phenomena involved (successive VOC oxidation steps, NO_x chemistry, compounds partitioning between several phases, SOA degradation, interactions between compounds in the particle, oligomerization).

The complexity of SOA formation makes chemical modeling of particulate matter (PM) difficult. To model SOA formation, most air quality models use simple parameterizations based on yields estimated from smog chamber measurements conducted under specific conditions, which can be different from atmospheric conditions (for example, oxidation under dry conditions). Those parameterizations rarely represent the effects of the NO_x level or oligomerization, whereas those effects have been shown to greatly affect the level of SOA predicted (e.g. Ng et al., 2007a,b; Pun and Seigneur, 2007). Therefore, it is necessary to develop a parameterization that gathers all those phenomena.

Isoprene (2-methylbutadiene) is the biogenic VOC, which has the largest emission rate of all the non-methane VOCs, estimated at 600 Tg yr⁻¹ (Guenther et al., 2006). Until recently, isoprene was believed not to be a major SOA precursor, despite its large emission flux, due in part to the high volatility of its first generation oxidation products such as



Correspondence to: F. Couvidat
(couvidaf@cerea.enpc.fr)

methacrolein and methyl vinyl ketone (Pandis et al., 1991). Furthermore, some smog chamber studies initially showed that no significant aerosol growth was observed from isoprene photooxidation under high-NO_x conditions (Pandis et al., 1991). However, during field studies in Amazonia, compounds like tetrols with the same carbon skeleton as isoprene were identified (Claeys et al., 2004; Edney et al., 2005), suggesting that isoprene could in fact contribute to SOA formation. SOA formation was then confirmed by several chamber studies and has been intensively investigated (Kroll et al., 2006; Surratt et al., 2006; Ng et al., 2008; Carlton et al., 2009; Jang et al., 2002).

Therefore, it is important to take isoprene-SOA into account in air quality modeling. Chamber experiments led to the identification of species composing isoprene SOA like tetrols and methylglyceric acid (Surratt et al., 2006; Kleindienst et al., 2009). As those products are rather small organic molecules (number of carbon atoms ≤ 5) and with numerous functional groups, they are expected to be highly hydrophilic. Then, those compounds would likely partition between an aqueous phase and the gas phase at high humidity in the atmosphere. It has been shown that taking into account the hydrophilic properties of isoprene SOA increases greatly the amount of SOA formed (Pun, 2008), whereas the parameterization of Zhang et al. (2007b) used currently in most air quality models does not take those effects into account.

The objective of this work is to develop a new model for the formation of SOA from isoprene, which takes into account NO_x chemistry, the hydrophilic properties of molecular species and oligomerization. First, a model is developed based on results from experiments conducted under dry conditions. Next, the model is extended to humid conditions by taking into account gas-aqueous phase partitioning.

2 Model development

2.1 Method

To develop the model for SOA formation from isoprene oxidation, the experimental results of Kroll et al. (2006) and Surratt et al. (2006) were used. Those experiments were done in the Caltech experimental chamber under both low-NO_x and high-NO_x conditions. A complete description of the facility is given by Cocker III et al. (2001). The gas-phase chemistry was simulated with RACM2 (Goliff and Stockwell, 2008), which includes a mechanism for isoprene oxidation. This mechanism has been shown to perform well for oxidant formation (Kim et al., 2009). The mechanism was modified to take into account the formation of the surrogate species to represent SOA formation as described below. The ROS2 algorithm (Verwer et al., 1999) was used to solve the chemical kinetic equations.

The experiments of Kroll et al. (2006) and Surratt et al. (2006) used blacklights, which emit in the ultraviolet be-

tween 300 and 400 nm with a maximum at 354 nm (Kroll et al., 2006). Under those conditions, nitrate radical (NO₃) and ozone (O₃) photolysis hardly occurs (Carter et al., 2005) and their photolysis rates are almost negligible. The rate given by Kroll et al. (2006) was used for H₂O₂ photolysis, which leads to hydroxy radical (HO) formation in the chamber. As the evolution of isoprene concentrations as a function of time was in good agreement with the isoprene degradation observed by Kroll et al. (2006), we consider that the HO concentrations are correctly simulated by the gas-phase mechanism and the impact of HO concentrations was not studied. The photolysis rate for NO₂ photolysis was chosen so that the maximum ozone concentration matches the results from Kroll et al. (2006). O₃, NO₃ and HONO photolysis rates were then calculated using the photolysis rates relative to NO₂ given by Carter et al. (2005).

As those experiments were done under dry conditions (RH < 10%), partitioning between the gas phase and an organic liquid phase was assumed. The partitioning was calculated using the model of Pankow (1994a,b), which defines the absorption equilibrium constant ($K_{p,i}$) according to Raoult's law as:

$$K_{om,i} = \frac{F_{i,om}}{A_i M_o} = \frac{760 R T}{MW_{om} 10^6 \zeta_i p_{L,i}^o} \quad (1)$$

where A_i is the gas-phase concentration of compound i (ng m⁻³), $F_{i,om}$ is the concentration of the compound i in the absorbing organic phase (ng m⁻³), M_o is the absorbing organic mass concentration (μg m⁻³), R is the ideal gas constant (8.206 × 10⁻⁵ m³ atm mol⁻¹ K⁻¹), T is the temperature (K), MW_{om} is the mean molecular weight of the absorbing organic phase (g mol⁻¹), ζ_i is the activity coefficient of compound i in the organic phase, and $p_{L,i}^o$ is the saturation vapor pressure of the absorbed compound (torr). The thermodynamic model UNIFAC (UNIversal Functional group Activity Coefficient) was used to calculate activity coefficients (Fredenslund et al., 1975). The missing UNIFAC parameters (for the functional groups nitrate and hydroperoxide) were taken from Comernolle et al. (2009). An iterative method was used to calculate activity coefficients and the partitioning.

The effect of temperature was taken into account according to the Clausius-Clapeyron equation using enthalpies of vaporization. Kleindienst et al. (2009) measured the effective enthalpies of vaporization of SOA formed from isoprene oxidation for both low-NO_x and high-NO_x conditions. Those values were used in this study: a value of 38.4 kJ mol⁻¹ for compounds formed under low-NO_x conditions (tetrols, hydroxy-hydroperoxides) and a value of 43.2 kJ mol⁻¹ for compounds formed under high-NO_x conditions (methylglyceric acid, organic nitrates). The use of experimental effective enthalpies of vaporization instead of theoretically estimated values for specific SOA compounds is appropriate because SOA surrogates may represent a lumping of several individual compounds.

Stoichiometric coefficients of condensable products, saturation vapor pressure (for low-NO_x conditions), effective partitioning constant (for high-NO_x conditions) of the different surrogate species were selected to reproduce the results of experiments. The reactions added to RACM2 for SOA formation from isoprene are listed in Table 1. The first six reactions dominate under low-NO_x conditions whereas the last two reactions dominate under high-NO_x conditions. Properties of surrogate species (molecular structure, saturation vapor pressures, molar mass and enthalpies of vaporization) are listed in Table 2.

The model development for SOA formation via oxidation of isoprene by NO₃ and HO is presented next. Although SOA formation occurs via oxidation of isoprene by O₃ (Kamens et al., 1982; Kleindienst et al., 2007; Nguyen et al., 2010), this pathway was not taken into account here because of insufficient quantitative and mechanism information to develop a model at this point.

2.2 Oxidation of isoprene by NO₃

The results of Ng et al. (2008) were used to model oxidation of isoprene by NO₃. In their study, a C₅-hydroxy-trinitrate (C₅H₉N₃O₁₀) compound (structure of the compound shown in Table 2) was found to be predominant in the “typical experiment” of Ng et al. (2008) (experiment relevant to atmospheric conditions). Therefore, it was used as a surrogate compound for SOA formation for oxidation by NO₃.

Isoprene reacts with NO₃ to form the surrogate ISON in RACM2 (which groups all compounds formed from the oxidation of isoprene with NO₃) by this reaction:



(with a kinetic constant $k = 6.61 \times 10^{-13} \text{ molecule}^{-1} \text{ cm}^3 \text{ s}^{-1}$). However, there is no oxidation of this compound by NO₃ in RACM2. The following reaction was added to RACM2 to take into account the formation of C₅-hydroxy-trinitrate:



where α_{NO_3} is the stoichiometric coefficient of the C₅-hydroxy-trinitrate. A kinetic constant of $7.0 \times 10^{-14} \text{ molecule}^{-1} \text{ cm}^3 \text{ s}^{-1}$ was taken from Rollins et al. (2009).

The method of Odum et al. (1996) with aerosol yields was used by Ng et al. (2008) with two surrogate compounds to estimate SOA formation parameters. Here, the same method was used but with only one surrogate compound because one surrogate compound is sufficient to reproduce the results of Ng et al. (2008) as shown in Fig. 1. A stoichiometric coefficient α_{NO_3} of 0.074 was estimated with a saturation vapor pressure of 1.12×10^{-6} torr.

It should be noted that the formation of C₅H₉N₃O₁₀ may be a minor pathway for SOA formation in the atmosphere because there is probably not enough NO₃ in the atmosphere

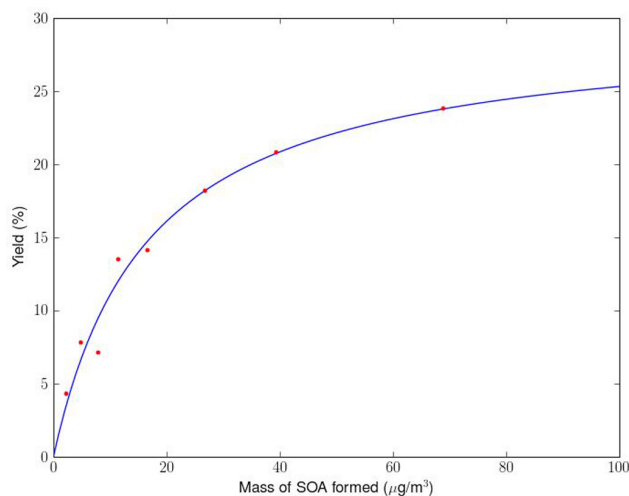


Fig. 1. SOA yield data and yield curve for isoprene-NO₃ reaction using one surrogate compound.

to form much C₅-hydroxy-trinitrate (C₅-dihydroxy-dinitrate is more likely). Reaction R2 could then overestimate SOA formation from ISON oxidation. However, this reaction could be used to deduce whether or not oxidation of isoprene by NO₃ can lead to a significant quantity of SOA. In this study, this reaction was used to make sure that NO₃ does not contribute significantly to SOA formation in environmental chambers.

2.3 Oxidation of isoprene by HO: formation of methyl-tetrols and hydroxy-hydroperoxides under low-NO_x conditions

Methyl-tetrols and hydroxy-hydroperoxides are expected to be the two main compounds formed from the photo-oxidation of isoprene under low-NO_x conditions. Whereas tetrols have been explicitly identified in chamber experiments (Kleindienst et al., 2009), the structure of hydroxy-hydroperoxides is still unknown and has not been conclusively identified (Kroll et al., 2006). Nevertheless, it is expected to be a key-component for SOA formation (Kroll et al., 2006; Surratt et al., 2006) and Surratt et al. (2006) confirmed that peroxides constitute a large fraction of SOA under low-NO_x conditions. Under the conditions of Kroll et al. (2006), the RO₂ (organic radical) chemistry is dominated by RO₂ + HO₂ reactions. Hydroxy-hydroperoxides are expected to be formed by those reactions. In RACM2, the formation of the radical (noted ISOP) from the oxidation of isoprene by HO can lead to the formation of first-generation hydroxy-hydroperoxides (noted ISHP) by the following chemical reactions:

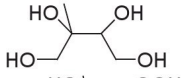
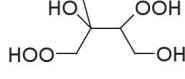
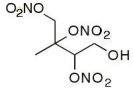
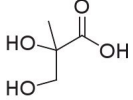
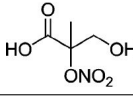


Table 1. Reactions and products added to RACM2.

Reactions	kinetic rate parameters ($\text{molecule}^{-1} \text{cm}^3 \text{s}^{-1}$)
ISHP + HO \Rightarrow ... + 0.28 BiPER + 0.030 BiDER	3.0×10^{-11}
2 ISOP \Rightarrow 2 MACR + HCHO + HO ₂ + 0.16 DIOL	2.0×10^{-12}
ISOP + MO ₂ \Rightarrow ... + 0.16 DIOL	$3.40 \times 10^{-14} \exp(221/T)$
ISOP + ACO ₃ \Rightarrow ... + 0.16 DIOL	$8.40 \times 10^{-14} \exp(221/T)$
DIOL + HO \Rightarrow 0.16 BiMT + HO*	1.30×10^{-10}
ISON + NO ₃ \Rightarrow 0.074 C ₅ H ₉ N ₃ O ₁₀	6.61×10^{-13}
MPAN + HO \Rightarrow ... + 0.063 BiMGA + 0.046 BiNGA	3.20×10^{-11}

* Oxidant HO is added as both reactant and product in order not to modify HO prediction by RACM2.

Table 2. Properties of the selected SOA surrogate species.

Surrogate species	Saturation vapor pressure (torr)	Molar Mass (g mol^{-1})	ΔH_{vap} (kJ mol^{-1})	Formula
BiMT	1.12×10^{-6} at 294 K	136	38.4	
BiPER ^a	2.61×10^{-6} at 298 K ^b	168	38.4	
BiDER	4.1×10^{-7} at 298 K ^b	136 ^b	38.4	unspecified
C ₅ H ₉ N ₃ O ₁₀	1.12×10^{-6} at 294 K	271	38.4	
BiMGA	1.40×10^{-5} at 298 K ^c	120	43.2	
BiNGA	1.39×10^{-5} at 298 K ^c	165	43.2	

^a Can undergo degradation due to photolytic reactions ($k_{\text{degradation}} = 2.0 \times 10^{-4} \text{s}^{-1}$).

^b Value obtained by using tetrols as BiDER structure. Results may change with another structure (change mainly due to different molar mass, see text).

^c Can undergo oligomerization. Calculated partitioning constant with this saturation vapor pressure has to be changed to take into account oligomerization with Eq. 3. $K_{\text{oligo}} = 64.2$.

However, the surrogate compound ISHP is too volatile to form SOA (the group contribution method SIMPOL.1 (Pankow and Asher, 2008) gives a saturation vapor pressure of 6.09×10^{-3} torr). Only one of the isoprene double bonds has been oxidized to form ISHP. If hydroxy-hydroperoxides SOA are formed, it can be assumed that ISHP is a key intermediate in their formation. So, it was assumed that hydroxy-hydroperoxides are formed from the oxidation of the ISHP double bond by HO and a subsequent RO₂ + HO₂ reaction:



where BiPER is a dihydroxy-dihydroperoxide, which may undergo photolysis, BiDER is another product with structure unknown, which is not photolyzed, α and β are respec-

tively the stoichiometric coefficients of BiPER and BiDER. Because of lack of data, molar mass and molecular structure of BiDER were assumed to be those of tetrols but the saturation vapor pressure was chosen to be different from the tetrol saturation vapor pressure in order to fit the experimental data (the sensitivity of the model to this assumption is investigated below). A rate constant of $3.0 \times 10^{-11} \text{molecule}^{-1} \text{cm}^3 \text{s}^{-1}$ was chosen for reaction R5 (kinetics supposed similar to the kinetics of the MACR + HO reaction in RACM2 Goliff and Stockwell, 2008).

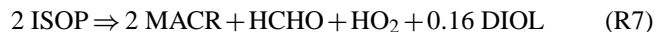
After reaching a maximum, the SOA mass was observed to decrease rapidly in the experiments of Kroll et al. (2006) under low-NO_x conditions. The decrease stopped immediately when the lights were turned off. It indicates that the loss is due to photolytic activity and not to wall losses. To our knowledge, rapid loss of SOA has not been observed in the photo-oxidation of another compound.

The mechanism for SOA loss has not been completely elucidated. The loss of SOA could be due to either gas-phase reactions (consumption of the partitioning compounds may drive equilibrium away from the particle phase) or particle-phase reactions (Kroll et al., 2006). For example, SOA loss could be due to gas-phase reaction with HO or photolysis. Kroll et al. (2006) assumed that the compounds accountable for the rapid SOA loss may be organic hydroperoxides as this loss is only seen under low-NO_x conditions. The pathway by which this SOA loss occurs should be clarified (particle-phase reaction, gas-phase reaction, photolysis) by further experimental studies.

Because of the uncertainties of the SOA loss mechanism, modeling the loss by a global BiPER degradation kinetics (degradation into both particulate and gas phases) was chosen:



Tetrols are assumed to be formed from the oxidation of diols which can be formed from RO₂ + RO₂ reactions. Under low-NO_x conditions, RO₂ + RO₂ reactions become predominant when concentrations of isoprene become high but can contribute slightly to SOA formation in Kroll et al. (2006). RACM2 does not take into account the diol formation from isoprene. However, Ruppert and Becker (2000) give a yield for diol formation between 7.1% and 9.3%. A yield of 8.0% was assumed here. Based on data of Ruppert and Becker (2000), a rate constant for the oxidation of diols by HO of $13.0 \times 10^{-11} \text{ molecule}^{-1} \text{ cm}^3 \text{ s}^{-1}$ was chosen. Under the conditions of Ruppert and Becker (2000), diols (noted here DIOL) can be expected to be formed from an ISOP + ISOP reaction, as follows:



The ISOP + ISOP reaction has been taken from Pöschl et al. (2000) and DIOL formation was added to this reaction (the yield was multiplied by two because two radicals from isoprene react in this reaction). ISOP can also be oxidized by radicals MO₂ and ACO₃. The following reactions have been added to RACM2:



where BiMT is the surrogate compound for tetrols and γ is the corresponding stoichiometric coefficient of BiMT. The

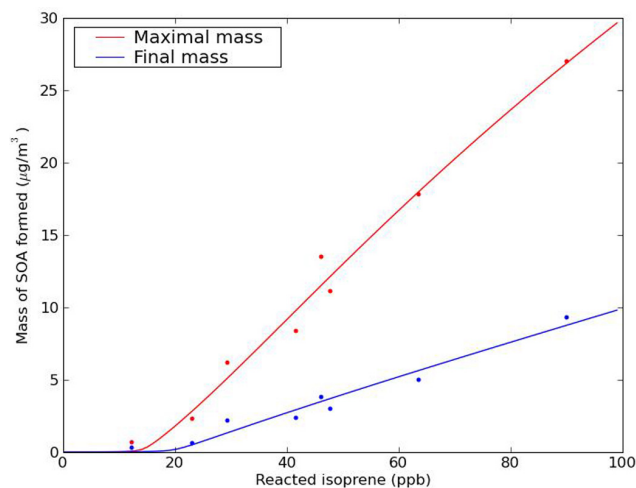


Fig. 2. SOA growth versus isoprene reacted. Dots correspond to measurements from Kroll et al. (2006). Lines correspond to results from the model for $T = 298 \text{ K}$.

group contribution method SIMPOL.1 gives similar saturation vapor pressures for tetrols and C₅-hydroxy-trinitrate. Accordingly, the saturation vapor pressure of tetrols was taken identical to that of C₅-hydroxy-trinitrate. A value for γ of 0.16 was used (assuming that the second oxidation has the same yield as the oxidation of the first double bond).

In the atmosphere, concentrations of ISOP are not typically sufficient for reaction R7 to be dominant. Inside environmental chambers, reactions R8 and R9 probably do not produce high quantity of DIOL due to the low concentrations of radicals MO₂ and ACO₃. However, those radicals are likely to be in higher concentrations in the atmosphere and BiMT could be formed by this pathway.

The stoichiometric coefficients α and β , the degradation rate of BiPER (R6) and the saturation vapor pressures of BiPER and BiDER were selected to minimize the error between modeled and experimental results by a least square method for both maximal and final mass of SOA. A mean temperature of 25 °C was assumed. However, to be able to solve the system, one of the parameters has to be set. According to Kroll et al. (2006), the SOA loss is about 0.006–0.018 min⁻¹. A mean value of 0.012 min⁻¹ was then taken for reaction R6. Optimization gives the values of the parameters presented in Table 3. Results of the comparison between modeled and measured SOA formation are shown in Table 4 and Fig. 2. Figure 3a shows the results of a simulation for 63.6 ppb of isoprene.

The model reproduces well the results from Kroll et al. (2006) but there are still uncertainties, in particular in the mechanism for SOA degradation and in the values for the yield and the saturation vapor pressure of methyl-tetrols. Under the conditions of Kroll et al. (2006), tetrols only represent a small part of SOA (simulation for the oxidation of

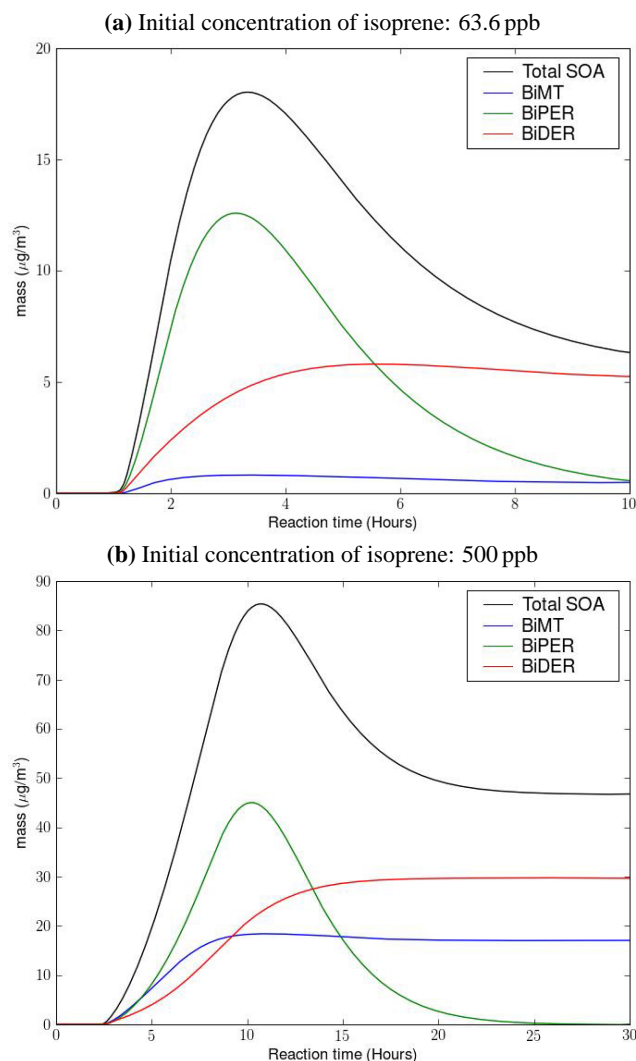


Fig. 3. Evolution of the calculated mass of SOA formed from isoprene photooxidation as a function of time at $T = 298$ K **(a)** for an initial isoprene concentration of 63.6 ppb **(b)** for an initial isoprene concentration of 500 ppb.

63.6 ppb of isoprene gives 8% of tetrols). But tetrols would represent a larger fraction of SOA with a larger quantity of oxidized isoprene because the ISOP + ISOP reaction would then be competitive with the ISOP + HO₂ reaction. This is confirmed by a simulation done with 500 ppb where tetrols represent about 40% of SOA formed (Fig. 3b).

2.4 Oxidation of isoprene by HO: formation of methyl-glyceric acid under high-NO_x conditions

Under high-NO_x conditions, Surratt et al. (2006) showed that methyl-glyceric acid (MGA) and its nitrate derivative can oligomerize and form substantial amount of SOA. Recent studies showed that MGA is formed from the oxidation of

Table 3. Values of the optimized parameters used for low-NO_x conditions at 298 K.

Parameter	Value
α	0.28
β	0.030
BiPER degradation	$2.0 \times 10^{-4} \text{ s}^{-1}$
BiPER saturation vapor pressure	$2.6 \times 10^{-6} \text{ torr}$
BiDER saturation vapor pressure	$4.1 \times 10^{-7} \text{ torr}$

MPAN (PAN-type molecule derived from the oxidation of methacrolein) (Surratt et al., 2010; Chan et al., 2010) and that MGA strongly depends on the initial [NO₂]/[NO] ratio (because MPAN formation is favored under high NO₂ conditions).

To model SOA formation under high-NO_x conditions, we assumed that SOA formation comes mainly from MGA and its nitrate derivative formation via MPAN oxidation. Currently, there is not enough information to distinguish MGA formation from its nitrate derivative formation in the model. However, experiments by Surratt et al. (2006) show that the two molecules are formed in equivalent quantities when isoprene is oxidized under high-NO_x conditions. We assumed that MPAN oxidation leads to the same overall mass (particle + gas) of MGA and its nitrate derivative. It means that there is 1.375 (molecular weight ratio of the two compounds) times as much MGA as nitrate:



where BiMGA represents MGA, BiNGA represents its nitrate derivative and λ is the stoichiometric coefficient for BiNGA. However, when methacrolein is directly oxidized, a higher quantity of nitrate derivative is formed. This fact could be due to faster MPAN formation when methacrolein is directly oxidized: more NO_x is available to react with MPAN, which leads to higher nitrate derivative concentrations. When isoprene is oxidized, methacrolein is formed first and MPAN formation occurs latter in the oxidation process. Then, there is more time for NO_x to be consumed to form HNO₃. As the nitrate derivative has a higher molecular weight than MGA and a priori a similar saturation vapor pressure, the hypothesis made could lead to underestimation of the SOA mass in environmental chamber under some conditions.

Oligomerization can impact strongly the formation of SOA (e.g. Gao et al., 2004; Jang et al., 2005; Liggió et al., 2005). It is then important to take it into account. To take into account oligomerization, a simple parameterization was developed:

$$K_{\text{oligo}} = \frac{A_{\text{oligomer}}}{A_{\text{monomer}}} \quad (2)$$

Table 4. Comparison of measured^a and modeled^b SOA formation (ΔM_o) for NO_x-free conditions: maximum ΔM_o and final ΔM_o .

Initial isoprene (ppb)	Measured ΔM_o (max) ($\mu\text{g m}^{-3}$)	Calculated ΔM_o (max) ($\mu\text{g m}^{-3}$)	Measured ΔM_o (final) ($\mu\text{g m}^{-3}$)	Calculated ΔM_o (final) ($\mu\text{g m}^{-3}$)
90.0	27.0 ± 0.5	26.9	9.3 ± 0.4	8.6
46.1	13.5 ± 0.6	11.5	3.8 ± 0.5	3.4
23.0	2.3 ± 0.5	2.8	0.6 ± 0.3	0.5
12.2	0.7 ± 0.1	0.07	0.3 ± 0.1	0.02
63.6	17.8 ± 0.5	18.0	5.0 ± 0.5	5.6
29.4	6.2 ± 0.8	5.1	2.2 ± 0.5	1.3
47.8	11.1 ± 0.5	12.2	3.0 ± 0.4	3.7
41.6	8.4 ± 0.4	9.8	2.4 ± 0.5	2.9

^a Measured values taken from Kroll et al. (2006).^b With $T = 298$ K.**Table 5.** Comparison of measured and modeled* SOA formation (ΔM_o) for high-NO_x conditions.

	Initial reagent (ppb)	Initial NO (ppb)	Initial NO ₂ (ppb)	Measured ΔM_o ($\mu\text{g m}^{-3}$)	Calculated ΔM_o ($\mu\text{g m}^{-3}$)
Kroll et al. (2006) (isoprene)	46.7	242	24	6.3 ± 1.0	6.0
	43.5	496	30	2.9 ± 1.2	3.3
	42.7	98	31	6.7 ± 1.3	5.9
	49.1	51	27	5.6 ± 1.3	7.0
	42.7	337	68	4.6 ± 1.0	4.7
Surratt et al. (2006) (isoprene)	42.0	708	37	1.7 ± 1.1	1.5
	500	827	34	74	90
	500	759	112	73	93
	500	805	87	104	92
	500	825	80	111	91
Surratt et al. (2006) (methacrolein)	500	891	74	95	90
	500	791	60	181	136
	500	898	30	197	121

* With $T = 298$ K and RH = 5%.

where K_{oligo} represents the ratio of the oligomer mass (A_{oligomer}) to the monomer mass (A_{monomer}). With this simple parameterization, an effective partitioning coefficient can be calculated as follows:

$$K_{\text{eff,om},i} = K_{\text{om},i}(1 + K_{\text{oligo}}) \quad (3)$$

where $K_{\text{om},i}$ is the absorption equilibrium constant of the monomer. It was calculated by using the saturation vapor pressures obtained with the SIMPOL.1 method for MGA and its nitrate derivative. The same parameter K_{oligo} was applied for both BiMGA and BiNGA.

The parameters λ and K_{oligo} were selected to minimize the error between the model and the results from Kroll et al. (2006) and Surratt et al. (2006) by a least-square method. A mean temperature of 298 K and a relative humidity of 5% were assumed. Optimization gives $\lambda = 0.046$ and $K_{\text{oligo}} =$

64.2. Results are presented in Table 5. Figure 4 shows the results of a simulation for 42.7 ppb of isoprene, 98 ppb of NO and 31 ppb of NO₂. The slight difference between the BiMGA and BiNGA concentrations is due to the slightly different activity coefficients of the two compounds.

The model successfully reproduces the results of Kroll et al. (2006) within the uncertainties of the experiments except for one experiment, (the lowest quantity of NO_x, the model gives a result ($7.0 \mu\text{g m}^{-3}$) close to the upper value, $6.9 \mu\text{g m}^{-3}$). This slight overestimation could be attributed to a calculated quantity of radical HO₂ too important or the fact that some reactions (the radical formed from ISHP + HO could react with NO and forms less SOA) are missing in the gas-phase mechanism. For high isoprene experiments, the model gives relative errors from 5 to 20%, but the model is less sensitive to NO_x conditions than observed in the

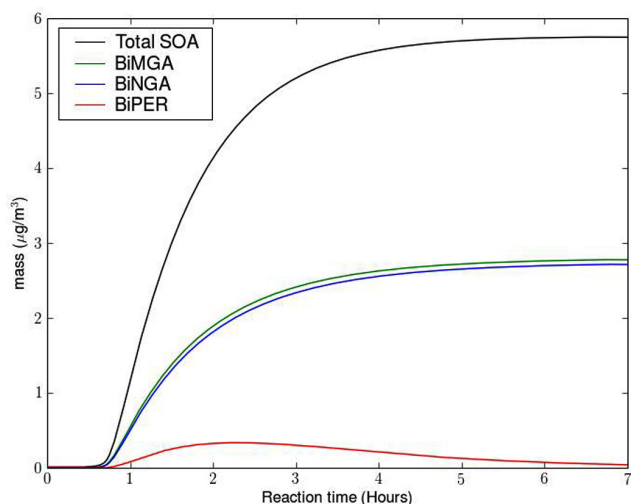


Fig. 4. Evolution of the calculated mass of SOA formed from the photooxidation of isoprene as a function of time for initial concentrations of 42.7 ppb of isoprene, 98 ppb of NO and 31 ppb of NO_2 at 298 K.

experiments. This lack of sensitivity of the model may be due to the fact that the BiMGA/BiNGA ratio in the model does not vary with NO_x conditions. It may also explain the underestimation of SOA formed when methacrolein is directly oxidized (which leads to a lower BiMGA/BiNGA ratio Surratt et al., 2006).

3 Influence of parameters

3.1 Influence of NO_x level and NO_2/NO ratio

Based on the experiments of Kroll et al. (2006), the SOA yield seems to be maximal for an oxidation of 300 ppb of NO_x and seems to decrease for higher concentrations. The recent study of Chan et al. (2010) shows that under high- NO_x conditions, the SOA yield strongly depends on the $[\text{NO}_2]/[\text{NO}]$ ratio due to MPAN chemistry (MPAN formation is favored under high NO_2 conditions).

To study the impact of the NO_x level, the amount of SOA formed was calculated as a function of initial NO_x concentrations (Fig. 5) for different $[\text{NO}_2]/[\text{NO}]$ initial ratios (the ratio may change with time). According to the model results, the amount of SOA decreases strongly only for low $[\text{NO}_2]/[\text{NO}]$ ratio (Fig. 5 for $[\text{NO}_2]/[\text{NO}] = 0.1$) and is below the amount of SOA formed in no- NO_x conditions ($3.5 \mu\text{g m}^{-3}$) for very high concentrations of NO_x (more than 500 ppb of NO_x for 45 ppb of oxidized isoprene and an initial $[\text{NO}_2]/[\text{NO}]$ ratio of 0.1). The inhibition of SOA formation for low $[\text{NO}_2]/[\text{NO}]$ ratios is due to the MPAN chemistry. Figure 4 shows that SOA begin to form nearly 1 h after the

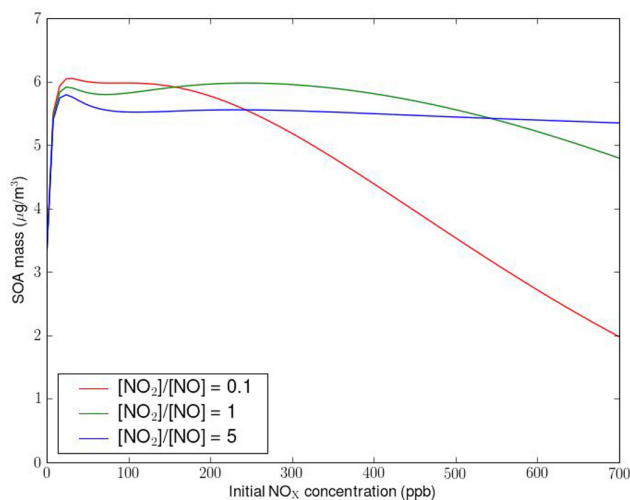


Fig. 5. Evolution of calculated SOA mass with NO_x for 45 ppb of oxidized isoprene and different initial $[\text{NO}_2]/[\text{NO}]$ ratios.

beginning of oxidation. To observe high concentration of SOA, MPAN formation must be favored after 1 h and so, a high $[\text{NO}_2]/[\text{NO}]$ ratio after 1 h must be observed. For an initial $[\text{NO}_2]/[\text{NO}]$ ratio of 0.1, the ratio after 1 h is: 53 for 100 ppb, 52 for 200 ppb, 31 for 300 ppb and 7 for 400 ppb. The decrease of SOA for a NO_x concentration greater than 200 ppb is due to the drop of NO_2 during oxidation.

For higher $[\text{NO}_2]/[\text{NO}]$ ratios, it seems that the SOA yield is higher under high- NO_x conditions than under low- NO_x conditions. For an initial $[\text{NO}_2]/[\text{NO}]$ ratio of 5, the quantity of SOA formed appears insensitive to the NO_x quantity. However, in reality, a stronger sensitivity may be observed if the BiMGA/BiNGA ratio were sensitive to NO_x concentrations.

For a $[\text{NO}_2]/[\text{NO}]$ ratio of 1, the final SOA yield (when there is no more SOA growth or loss) was calculated as a function of initial isoprene concentration for several initial concentrations of NO_x (Fig. 6). For the no- NO_x simulation, the yield increases and stabilizes at about 3.75%. In this case, a typical SOA yield curve is obtained. For high- NO_x simulations, the evolution of the yield is more complex because of the MPAN chemistry. Yields can vary from 5 to 7% if more than 100 ppb of isoprene is oxidized. For 300 ppb of NO_x , the yield decreases slightly between 300 and 400 ppb of oxidized isoprene and increases for higher concentrations of isoprene.

It is difficult to deduce a general pattern for isoprene SOA formation in presence of NO_x because of the complex effects of the gas-phase chemistry. Depending on NO_x concentrations and the $[\text{NO}_2]/[\text{NO}]$ ratio, the yield can be lower or as much as twice higher than the no- NO_x SOA yield. However, for atmospheric conditions (NO_x and isoprene concentrations generally inferior to 100 ppb), the yield should be

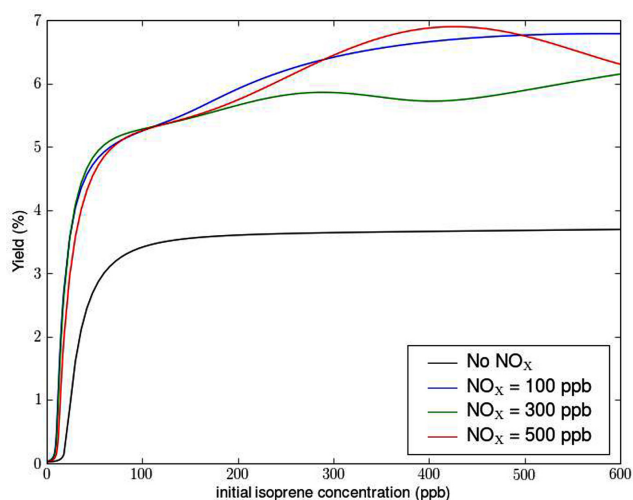


Fig. 6. Evolution of calculated yield with isoprene concentration for different NO_x concentrations with a $[\text{NO}_2]/[\text{NO}]$ ratio of 1.

higher under high- NO_x conditions than under low- NO_x conditions, when SOA formation occurs in an organic phase.

3.2 Influence of temperature

Figure 7 shows the effect of temperature on the amount of SOA formed for different $[\text{NO}_2]/[\text{NO}]$ ratios. In all cases, a decrease of the temperature by 20°C leads to an increase of SOA mass by about $2\ \mu\text{g m}^{-3}$. This result can be explained by an increase in SOA volatility when the temperature increases. The temperature affects SOA partitioning more than the kinetics of the reactions leading to the formation of SOA. However, the activation energy was not used for all the reactions due to a lack of data and the chemical kinetics could be in reality more sensitive to temperature.

3.3 Influence of the BiDER molecular structure

To investigate the impact of the BiDER molecular structure (which could be very different from the structure of tetrols) on the results of the model optimization, we substitute its structure by that of another compound. We used the peroxy-hemiacetal that could be formed by the particle phase reaction (Kroll and Seinfeld, 2008) of a trihydroxyhydroperoxide with glyoxal. This compound has a molar mass of $224\ \text{g mol}^{-1}$ (instead of $136\ \text{g mol}^{-1}$ for tetrols). Using this compound, the optimization gives the same yield for BiPER (0.28) but a slightly different saturation vapor pressure (2.2×10^{-6} torr instead of 2.6×10^{-6} torr). Results obtained for BiPER are not very sensitive then to the choice of the BiDER structure. The results obtained by assuming that BiDER has the structure of tetrols should give a good estimation of BiPER yield and saturation vapor pressure.

For BiDER, the molar yield is lower (0.018 instead of 0.030 but the mass yield is the same) and the saturation vapor pressure is lower (2.5×10^{-7} torr instead of 4.1×10^{-7} torr). Therefore, BiDER volatility may be underestimated in the model.

4 Extension of the model to humid conditions

The model described above applies to dry conditions. However, it is important to implement in an air quality model an SOA model that covers the full range of atmospheric conditions including high humidity conditions. Consequently, a parameterization for SOA formation must take into account humid conditions. Moreover, the SOA compounds produced from isoprene photooxidation may be highly hydrophilic due to their structural composition, i.e., short compounds (number of carbons ≤ 5) with several functional groups. Under humid conditions, in presence of both an aqueous phase and an organic liquid phase, isoprene SOA surrogates may partition mostly between the aqueous phase and the gas phase rather than the organic phase and the gas phase.

Several methods have been used to account for the influence of water on SOA formation. On one hand, one can treat the atmospheric particles as internal mixtures (all particles of a same size have the same chemical composition) and solve the thermodynamics with possible phase separation (e.g., mostly organic and aqueous phases) as performed by Pun (2008) and Zuend et al. (2010). On the other hand, one can treat the atmospheric particles as external mixtures with aqueous (mostly inorganic) particles being distinct from hydrophobic (mostly organic) particles as performed by Pun et al. (2002, 2006). The latter approach is used here.

For the extension to humid conditions, a parameterization for the partitioning between the gas phase and the aqueous phase was added to the model described above. It was assumed that all surrogate SOA compounds can partition between the gas phase and any liquid phase (aqueous phase and organic phase). Surratt et al. (2010) showed that under low- NO_x conditions, an epoxidol intermediate should be formed from reaction R5 with a high yield (about 75%). This epoxidol can lead to methyl-tetrol and other components formation in the presence of an acid aerosol. However, the study of aqueous-phase reactions (Ervens et al., 2008; Volkamer et al., 2009) was considered outside the scope of this work and was not modeled here.

4.1 Parameterization of the partitioning between an aqueous phase and the gas phase

To extend the model to humid conditions, the partitioning between the gas phase and the aqueous phase is calculated with a modified Henry's law (Pun et al., 2002):

$$H_i = \frac{A_i \zeta_i}{M_i \text{LWC } p_i} \quad (4)$$

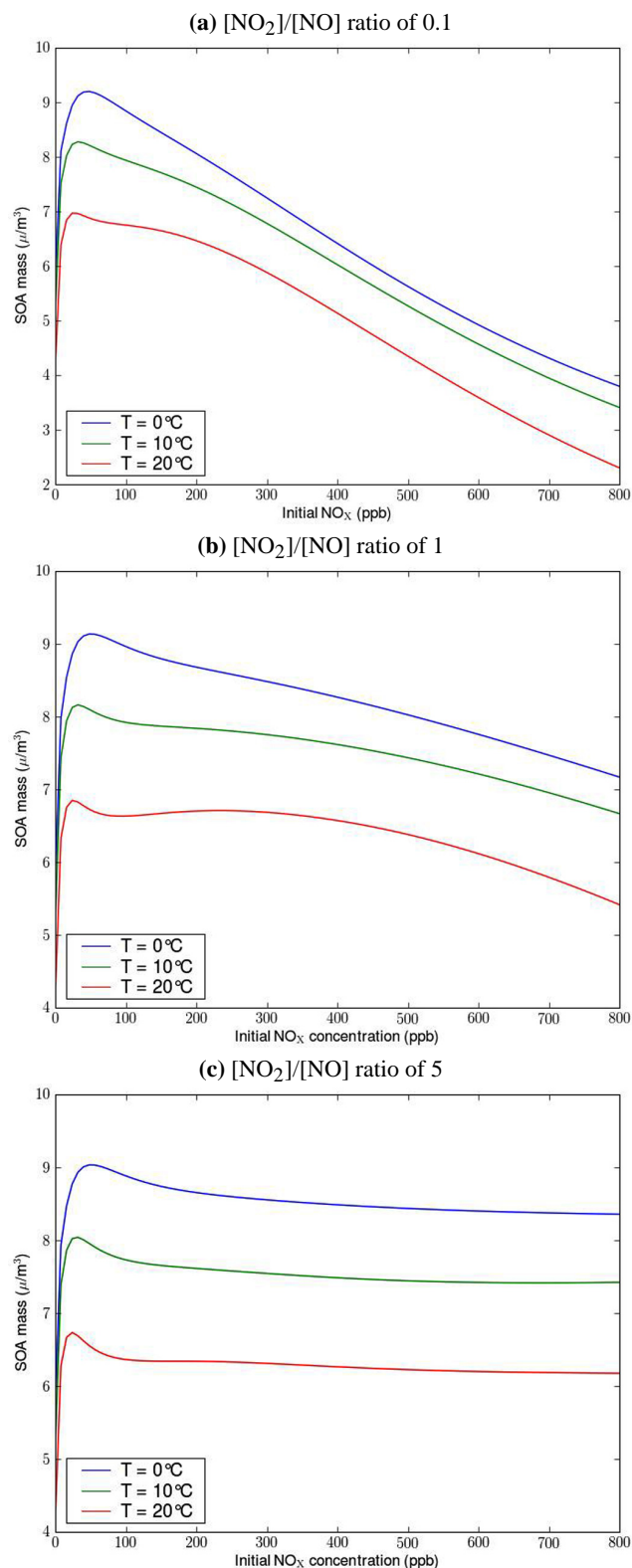


Fig. 7. Evolution of SOA with NO_x for 45 ppb of oxidized isoprene at different temperatures for: (a) $[\text{NO}_2]/[\text{NO}]$ ratio of 0.1, (b) $[\text{NO}_2]/[\text{NO}]$ ratio of 1, (c) $[\text{NO}_2]/[\text{NO}]$ ratio of 5.

with H_i the Henry's law constant of compound i ($\mu\text{M atm}^{-1}$), p_i the partial pressure of compound i in the gas phase (atm), LWC the liquid water content ($L_{\text{water}} \text{ m}^{-3}$ of air), M_i the molar mass of compound i and ζ_i the activity coefficient of compound i in the aqueous phase defined by reference to the infinite dilution. ζ_i can be computed by using the UNIFAC model:

$$\zeta_i = \frac{\gamma_i}{\gamma_i^\infty} \quad (5)$$

where γ_i is the activity coefficient of the compound i in the aqueous phase computed with UNIFAC and γ_i^∞ is the activity coefficient of compound i at infinite dilution computed with UNIFAC.

Different methods can be used to determine the Henry's law constant. Functional group methods give very high values for the Henry's law constant of BiMT ($2.7 \times 10^{16} \text{ M atm}^{-1}$ and $1.66 \times 10^{16} \text{ M atm}^{-1}$ with the methods of Meylan and Howard (2000) and Suzuki et al. (1992) respectively). On the contrary, the HENRYWIN bond contribution method of Meylan and Howard (2000, 1991) predicts a lower value for BiMT: $2.45 \times 10^6 \text{ M atm}^{-1}$. However, according to the data available in Raventos-Duran et al. (2010), the HENRYWIN bond contribution method seems to underestimate the Henry's law constant for compounds with several hydroxy groups (for example, for propane-1,3-diol, this method predicts a Henry's law constant of $6.31 \times 10^3 \text{ M atm}^{-1}$ whereas the experimental value is $1.0 \times 10^6 \text{ M atm}^{-1}$). SPARC online (Hilal et al., 2008) seems then to provide the best estimation for Henry's constants ($3.38 \times 10^{10} \text{ M atm}^{-1}$ for BiMT and $5.25 \times 10^8 \text{ M atm}^{-1}$ for BiMGA). However, SPARC online does not provide algorithms to calculate the Henry's law constants of the other compounds.

We chose to calculate the other Henry's law constants by reference to either BiMT or BiMGA using the following equation:

$$H_i = \frac{\gamma_j^\infty P_j^0}{\gamma_i^\infty P_i^0} H_j \quad (6)$$

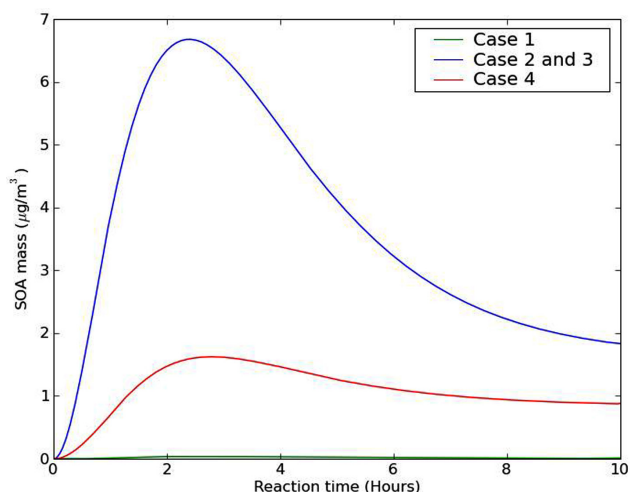
where j is the compound of reference (BiMT or BiMGA) and i is the compound for which the Henry's law constant is wanted. The Henry's law constants for BiPER, BiDER and $\text{C}_5\text{H}_9\text{N}_3\text{O}_{10}$ were calculated by reference to BiMT. The Henry's law constant for BiNGA was calculated by reference to BiMGA. The saturation vapor pressures used in the model for dry conditions were used for the calculation. The calculated values at 298 K are presented in Table 6.

4.2 Influence of an aqueous phase on SOA formation

The partitioning of the surrogate compounds under atmospheric conditions was calculated for four different cases. In the first case, SOA partition between the gas phase and

Table 6. Calculated Henry's law constants for SOA surrogate species.

Surrogate species	H_i at 298 K ($M \text{ atm}^{-1}$)
BiMT	3.30×10^{10}
$C_5H_9N_3O_{10}$	4.75×10^6
BiMGA	5.25×10^8
BiNGA	3.73×10^7
BiPER	8.09×10^9
BiDER	8.91×10^{10}

**Fig. 8.** Effect of an aqueous phase on SOA formation under no- NO_x conditions for 10 ppb of initial isoprene concentration for different cases. Case 1: Condensation on $5 \mu\text{g m}^{-3}$ of POA. Case 2: Condensation on $50 \mu\text{g m}^{-3}$ of liquid water. Case 3: Condensation on $5 \mu\text{g m}^{-3}$ of POA and on $50 \mu\text{g m}^{-3}$ of liquid water. Case 4: Condensation on $5 \mu\text{g m}^{-3}$ of an ideal organic phase.

an organic phase constituted by primary organic aerosols (POA). A mean value of $5 \mu\text{g m}^{-3}$ for POA concentrations was chosen as follows: 40% of $C_{23}H_{47}COOH$, 5% of $C_8H_{17}CH=CHC_7H_{14}COOH$, 15% of 4-(2-propio)-syringone, 12% of $C_{29}H_{60}$ and 28% of 2-carboxybenzoic acid (EPRI, 1999). In the second case, SOA partition between the gas phase and an aqueous phase. A value of $50 \mu\text{g m}^{-3}$ of liquid water was used in the second case. The aqueous aerosol was supposed to be too acid for BiMGA and BiNGA to dissociate. In the third case, SOA can condense on $5 \mu\text{g m}^{-3}$ of POA and on $50 \mu\text{g m}^{-3}$ of liquid water. In the fourth case, surrogates can condense on an organic phase assumed to be ideal (activity coefficients equal to 1).

Under no- NO_x conditions ($[\text{NO}] = [\text{NO}_2] = 0.0$), no substantial amount of SOA is formed in the first case (maximum of SOA formed is $0.027 \mu\text{g m}^{-3}$) whereas a significant amount is formed in the second case. The low amount of SOA

formed in the first case is due to low affinity of the surrogate compounds formed under those conditions (mainly BiPER and BiDER) with POA. In the second and third case, the same amount of SOA is formed (because all SOA compounds seem to partition only in the aqueous phase). Figure 8 shows the evolution of SOA formed for the second and third cases. A substantial amount of isoprene is formed ($1.6 \mu\text{g m}^{-3}$ at the end of the oxidation and a maximum at $6.7 \mu\text{g m}^{-3}$). The amount of SOA formed is even greater than in the case where SOA would condense on an ideal organic phase, which gives much greater concentrations than the non-ideal organic phase case. This result shows the importance of taking into account the non-ideality of particles for SOA partitioning. Furthermore, SOA formed from isoprene photooxidation under low- NO_x conditions are not likely to condense on POA (due to non-ideality of the organic phase), it would more likely condense efficiently on an aqueous phase. It should be noted that, whereas surrogates do not condense on POA, they condense almost entirely on the aqueous phase (only 1% of BiPER remains in the gas phase).

Under high- NO_x conditions ($[\text{NO}] = [\text{NO}_2] = 50$ ppb), all the components formed are not highly hydrophilic. Figure 9 shows the quantity of SOA formed for the different cases under high- NO_x conditions. There is still a lower quantity of SOA ($0.16 \mu\text{g m}^{-3}$) formed when SOA condense on POA than when they condense on an aqueous phase ($0.59 \mu\text{g m}^{-3}$). But, contrary to the low- NO_x conditions, the third case shows that a non-negligible part of the surrogates condense on the organic phase. The fourth case (ideal organic phase) strongly increases the mass of SOA. The difference between low- NO_x and high- NO_x conditions is due to lower Henry's law constants of the surrogate species, which dominate under high- NO_x conditions. Whereas, the measured SOA yield was higher for dry conditions under high- NO_x conditions (but for concentrations of NO_x less than 300 ppb) than under low- NO_x conditions, it is possible that in the atmosphere under high- NO_x conditions, less SOA could be formed due to lower water solubility of the corresponding SOA. The increase in SOA mass under humid conditions is commensurate with the results obtained by Pun (2008) who estimates, using a different approach, an increase by a factor of five of SOA mass by taking into account the hydrophilic properties of SOA from isoprene.

To explain the absorption of surrogates in the organic phase in high- NO_x but not in low- NO_x , the distribution of the SOA (formed from the oxidation of 10 ppb of isoprene with 50 ppb of NO and NO_2) between the organic and aqueous phases for different $M_{\text{water}}/M_{\text{organic}}$ ratios is shown in Fig. 10. BiMT, BiPER and BiDER (compounds formed under low- NO_x conditions) are only present in the aqueous phase and do not condense significantly in the organic phase. BiMGA (formed under high- NO_x) does not condense on the aqueous as efficiently as the surrogates formed under low- NO_x conditions. However, for an $M_{\text{water}}/M_{\text{organic}}$ ratio of 1.60% of particulate BiMGA is in the aqueous phase and around 95%

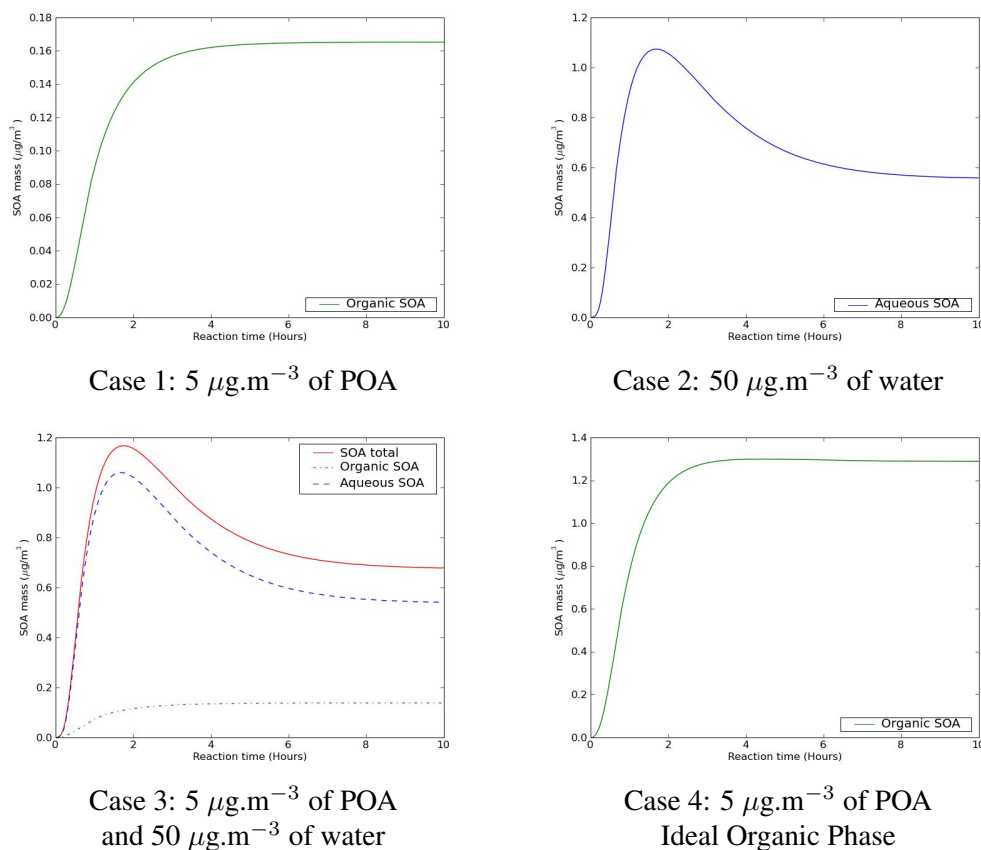


Fig. 9. Effect of an aqueous phase on SOA formation under high- NO_x conditions ($[\text{ISO}] = 10$ ppb, $[\text{NO}] = [\text{NO}_2] = 50$ ppb). Case 1: Condensation on $5 \mu\text{g m}^{-3}$ of POA. Case 2: Condensation on $50 \mu\text{g m}^{-3}$ of liquid water. Case 3: Condensation on $5 \mu\text{g m}^{-3}$ of POA and on $50 \mu\text{g m}^{-3}$ of liquid water. Case 4: Condensation on $5 \mu\text{g m}^{-3}$ of an ideal organic phase.

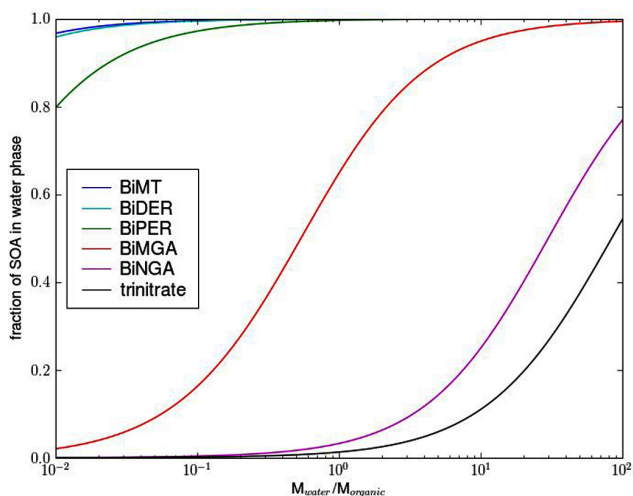


Fig. 10. Distribution of the absorbed surrogates between the aqueous phase and the organic phase for different $M_{\text{water}}/M_{\text{organic}}$ ratios if oligomerization only happens in the organic phase.

for a ratio of 10. When, the $M_{\text{water}}/M_{\text{organic}}$ ratio is superior to 1 in the atmosphere, BiMGA should partition preferably between the aqueous phase and the gas phase. BiNGA and C_5 -hydroxy-trinitrate seem to be hydrophobic because even for an $M_{\text{water}}/M_{\text{organic}}$ ratio of 10, they condense preferably on the organic phase. The condensation of SOA on the organic phase under high- NO_x conditions is then due to the hydrophobic properties of BiNGA (only a small quantity of C_5 -hydroxy-trinitrate is formed under the conditions considered here).

The AER/EPRI/Caltech model (AEC) (Pun et al., 2002, 2003, 2006) is a model for SOA formation that takes into account the hydrophilic and hydrophobic properties of surrogates. It distinguishes compounds into two types: hydrophilic compounds (which are absorbed only in an aqueous particle) and hydrophobic compounds (which are absorbed only in an organic particle). In AEC, a compound cannot condense on both phases simultaneously; we investigate here the uncertainty associated with this formulation. According to the distribution of the surrogates, BiMT, BiPER, BiDER and BiMGA may be considered hydrophilic compounds and BiNGA and $\text{C}_5\text{H}_9\text{N}_3\text{O}_{10}$ hydrophobic compounds. Under

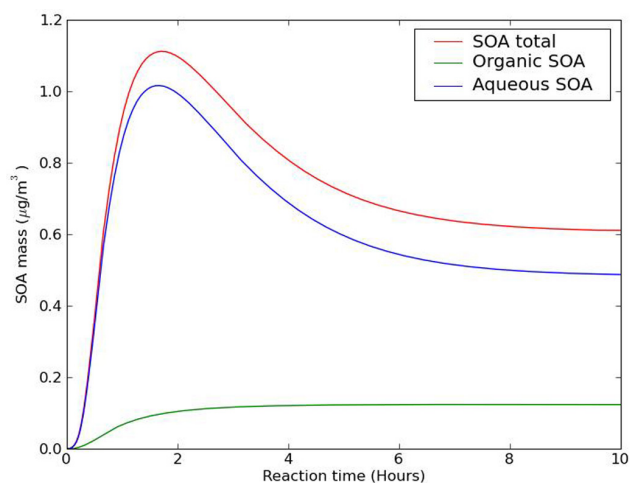


Fig. 11. Simulated SOA concentration in aqueous and organic phases for 10 ppb of isoprene and high-NO_x conditions ([NO] = [NO₂] = 50 ppb) assuming all the surrogates are hydrophilic except for BiNGA and C₅H₉N₃O₁₀.

low-NO_x conditions, as the compounds formed are highly hydrophilic and condense almost entirely on aqueous particles, the hypothesis of AEC does not change the results significantly. Figure 11 shows the evolution of SOA formed with time for the high-NO_x case, assuming that surrogates are only hydrophilic or only hydrophobic. The difference between the case where all compounds can partition among all the phases (see Fig. 9) and the case with the hypothesis of AEC is greater for high-NO_x conditions because BiMGA and BiNGA (major components formed under high-NO_x conditions) are neither totally hydrophilic nor hydrophobic. In this case, the mass of SOA is underestimated by the AEC hypothesis by 11%: 0.61 µg m⁻³ (Fig. 11) with the AEC hypothesis against 0.68 µg m⁻³ (Fig. 9) without the AEC hypothesis.

4.3 Influence of oligomerization and particle pH on partitioning

SOA surrogates have been separated between hydrophobic and hydrophilic compounds, however, calculated partitioning can change whether oligomerization is taken into account in the computation or not. We assumed that esterification does not occur in the aqueous phase, although Altieri et al. (2008) observed formation of oligoesters in an aqueous phase. Additional absorption of acidic SOA species (BiMGA and BiNGA) occurs by dissociation in an aqueous phase. For a pH superior to pK_a (pK_a = 4 estimated for BiMGA with SPARC online), BiMGA and BiNGA would, therefore, dissociate and would be more efficiently absorbed. On the other hand, oligomerization in the organic phase could be less important in the atmosphere due to less concentrated monomers. The amount of SOA formed (for 10 ppb of iso-

prene, 50 ppb of NO, 50 ppb of NO₂, 5 µg m⁻³ of POA and 50 µg m⁻³ of liquid water) was simulated to investigate the sensitivity of the system to additional absorption due to acid dissociation and oligomerization.

To investigate the effect of potential oligomerization in the aqueous phase and pH, an effective Henry's law constant for BiMGA and BiNGA was used:

$$H_{\text{eff},i} = H_i(1 + K_{\text{oligo}}) \quad (7)$$

where K_{oligo} is the same constant as the one in Eq. 3 (it supposes that additional absorption due to dissociation and oligomerization occurs with the same extent in both phases). Figure 12a shows the evolution of the SOA mass. Additional absorption of BiMGA and BiNGA greatly increases the amount of SOA formed (1.7 µg m⁻³ against 0.68 µg m⁻³ without additional absorption). Moreover, there is almost no condensation on POA: all the condensation occurs on the aqueous phase. Figure 13a shows the distribution of the surrogates between the two condensed phases for different $M_{\text{water}}/M_{\text{organic}}$ ratios. For an $M_{\text{water}}/M_{\text{organic}}$ ratio of 1, almost all the particulate BiMGA is in the aqueous phase and nearly 80% of the particulate BiNGA is in the aqueous phase. Contrary to the case where there is no additional absorption in the aqueous phase (see Fig. 10), BiNGA can then be considered hydrophilic when its additional absorption is accounted for.

To investigate the possible absence of oligomerization in the organic phase, $K_{\text{oligo}} = 0$ was used. Figure 12b shows the evolution of the SOA mass without oligomerization in the organic phase. The final SOA mass is reduced by 16% (0.57 µg m⁻³ without oligomerization against 0.68 µg m⁻³ with oligomerization). There is no significant absorption of the surrogates on the organic phase. Figure 13b shows the distribution of the surrogates between the two phases. As in the previous case, BiNGA partitions more efficiently between the aqueous phase and the gas phase and can be considered hydrophilic when its oligomerization in the organic phase is not accounted for.

Whether BiNGA condenses on POA or an aqueous phase depends on potential additional absorption in the aqueous phase by potential oligomerization and dissociation and on the extent of oligomerization in the organic phase. Most of the components can be classified as hydrophilic (BiMT, BiPER, BiDER and BiMGA) but BiNGA can be considered either as hydrophobic or hydrophilic, depending on oligomerization in the organic phase or additional absorption in the aqueous phase.

4.4 Sensitivity of the model to Henry's law constants

One of the main uncertainties of the model is the values of Henry's law constants. The constants used here were estimated using the saturation vapor pressure and the activity coefficient at infinite dilution; however, as discussed above,

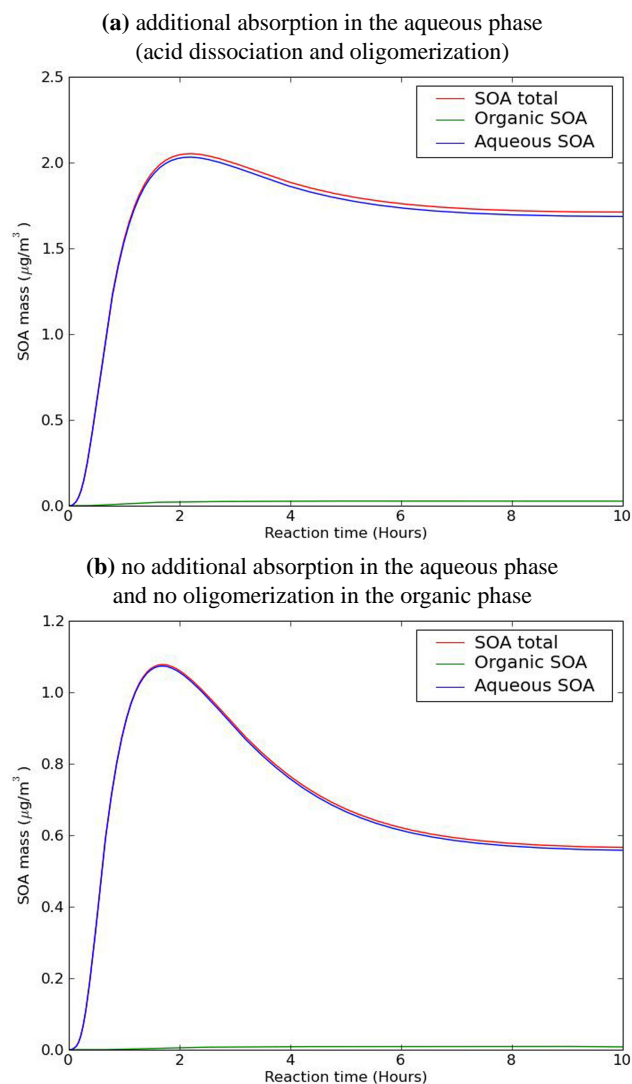


Fig. 12. Evolution with time of the mass of SOA formed: (a) with additional absorption in the aqueous phase (acid dissociation and oligomerization) and (b) with no additional absorption in the aqueous phase and no oligomerization in the organic phase.

other methods may lead to quite different results. For that reason, a sensitivity study was conducted to evaluate the impact of those uncertainties on liquid-gas partitioning.

Under low- NO_x conditions, the partitioning is not very sensitive to the values. If Henry's law constants are divided by 2, $1.76 \mu\text{g m}^{-3}$ of SOA are formed instead of $1.83 \mu\text{g m}^{-3}$ (for $50 \mu\text{g m}^{-3}$ of liquid water and 10 ppb of initial isoprene). If the Henry's law constants are divided by 10, $0.92 \mu\text{g m}^{-3}$ is formed (i.e. half of SOA previously formed). On the contrary, when Henry's law constants are multiplied by 10, the quantity of SOA does not change significantly ($1.86 \mu\text{g m}^{-3}$ instead of $1.83 \mu\text{g m}^{-3}$) because most of the SOA species are already present in the condensed phase. So, for BiMT, BiPER and BiDER, the amount of

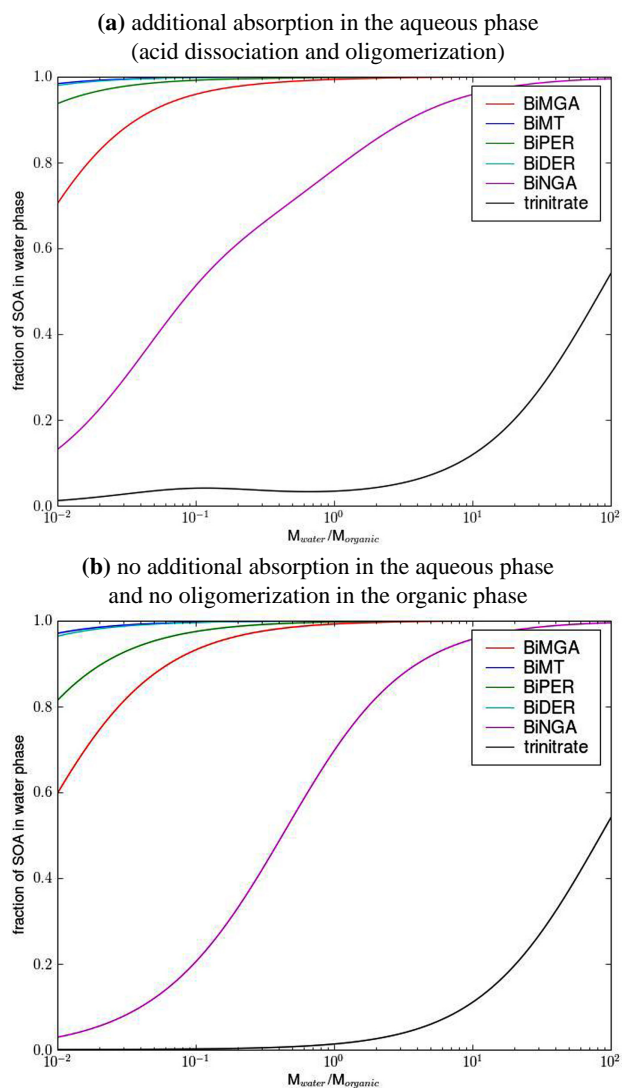


Fig. 13. Distribution of the absorbed surrogates between the aqueous phase and the organic phase for different $M_{\text{water}}/M_{\text{organic}}$ ratios: (a) with additional absorption in the aqueous phase (acid dissociation and oligomerization) and (b) with no additional absorption in the aqueous phase and no oligomerization in the organic phase.

SOA formed does not change significantly for a small decrease of the Henry's law constants or for an important increase of the Henry's law constant. Of course, the impact of Henry's law constant values is more important for lower quantity of liquid water, but even at $5 \mu\text{g m}^{-3}$ of liquid water, Henry's law constant values have a small impact on SOA formation: $1.46 \mu\text{g m}^{-3}$ of SOA for Henry's law constants divided by two, and $1.86 \mu\text{g m}^{-3}$ for Henry's law constants multiplied by ten instead of $1.73 \mu\text{g m}^{-3}$. If the structure of the peroxy-hemiacetal that could be formed by the particle phase reaction (Kroll and Seinfeld, 2008) of a trihydroxyhydroperoxide with glyoxal, the Henry's law constant of BiDER should be higher (less volatile and more affinity with

water) by about a factor 4. But, as the formation of SOA is not very sensitive to Henry's law constants, the impact of the uncertainty of the BiDER structure should be limited.

Under high-NO_x conditions, the partitioning is more sensitive. However, it was shown previously that using effective Henry's law constants taking into account additional absorption due to oligomerization and dissociation greatly influences the partitioning of the surrogates. The main uncertainty for BiMGA and BiNGA partitioning is then the extent of the additional absorption rather than the actual Henry's law constants for BiMGA and BiNGA.

For C₅H₉N₃O₁₀ formed by oxidation of isoprene by NO₃ radicals, as the component seems hydrophobic, the value of its Henry's law constant does not impact its partitioning noticeably.

5 Conclusions

A model for SOA formation from isoprene oxidation that takes into account different chemical regimes and the hydrophilic properties of SOA has been developed. For low-NO_x conditions, SOA was found to be highly hydrophilic and it is likely that components formed would condense on an aqueous phase rather than on an organic phase. For high-NO_x conditions, methyl glyceric acid (BiMGA) was found to be hydrophilic whereas the nitrate derivative (BiNGA) can be considered as hydrophilic or hydrophobic depending on the hypothesis formulated.

A major conclusion is the importance of the hydrophilic properties of SOA formed from isoprene oxidation. Because the parameterizations derived from smog chambers experiments apply to dry conditions, SOA formation could be underestimated in current models.

This SOA model can be implemented in an air quality model to evaluate the amount of isoprene-SOA formed in the atmosphere. However, several questions remain before implementing this model. Are all the pathways described here important for SOA formation? The formation of C₅-hydroxy-trinitrate may not be relevant in the atmosphere and in any case, it could be a minor pathway for the formation of SOA in the atmosphere. If 3-D simulations show that those compounds do not contribute significantly to the SOA burden, this pathway could be removed from the model. Can the number of surrogates be reduced? Some surrogates like BiMT and BiDER have similar thermodynamic properties (same molecular structure and high Henry's law constants), and they could perhaps be merged into a single surrogate.

To develop this model, several assumptions were made. Readers should be aware of these assumptions and that several uncertainties remain. Which molecular structure for BiDER should be chosen? Can the products formed in experimental chambers be formed under all conditions in the atmosphere? For example, if BiDER is formed by reaction in an organic phase, it is possible that it is not formed when

the compounds tend to condense on liquid water. To what extent does the oligomerization occur in the atmosphere for BiMGA and BiNGA. Are the estimated Henry's law constants and saturation vapor pressures reliable enough for extrapolation to atmospheric conditions? For example, Barley and McFiggans (2010) showed that results of models of SOA formation are very sensitive to saturation vapor pressures.

It should be noted that the main uncertainties of the model concern the high-NO_x regime. However, isoprene is emitted by biogenic sources in remote areas where concentrations of NO_x are low. Most of SOA should, therefore, be formed under low-NO_x conditions and the impact of the uncertainties of the high-NO_x regime should be limited.

Acknowledgements. This work was funded in part by ADEME, the French Agency for the Environment and Energy Management. Thanks are due to Nathalie Poisson, ADEME, Jean-François Doussin, LISA, Université Paris-Est, and Anne Monod, Laboratoire Chimie Provence, Université Aix-Marseille for useful discussions.

Edited by: H. Saathoff

References

- Altieri, K., Seitzinger, S., Carlton, A., Turpin, B., Klein, G., and Marshall, A.: Oligomers formed through in-cloud methylglyoxal reactions: chemical composition, properties, and mechanisms investigated by ultra-high resolution FT-ICR Mass Spectrometry, *Atmos. Environ.*, 42, 1476–1490, doi:10.1016/j.atmosenv.2007.11.015, 2008.
- Barley, M. H. and McFiggans, G.: The critical assessment of vapour pressure estimation methods for use in modelling the formation of atmospheric organic aerosol, *Atmos. Chem. Phys.*, 10, 749–767, doi:10.5194/acp-10-749-2010, 2010.
- Carlton, A. G., Wiedinmyer, C., and Kroll, J. H.: A review of Secondary Organic Aerosol (SOA) formation from isoprene, *Atmos. Chem. Phys.*, 9, 4987–5005, doi:10.5194/acp-9-4987-2009, 2009.
- Carter, W., Cocker III, D., Fitz, D., Malkina, I., Bumiller, K., Sauer, C., Pisano, J., Bufalino, C., and Song, C.: A new environmental chamber for evaluation of gas-phase chemical mechanisms and secondary aerosol formation, *Atmos. Environ.*, 39, 7768–7788, doi:10.1016/j.atmosenv.2005.08.040, 2005.
- Chan, A., Chan, M., Surratt, J., Chhabra, P., Loza, C., Crounsoe, J., Yee, L., Flagan, R., Wennberg, P., and Seinfeld, J.: Role of aldehyde chemistry and NO_x concentrations in secondary organic aerosol formation, *Atmos. Chem. Phys. Discuss.*, 10, 10219–10269, doi:10.5194/acpd-10-10219-2010, 2010.
- Claeys, M., Graham, B., Vas, G., Wang, W., Vermeylen, R., Pashynska, V., Cafmeyer, J., Guyon, P., Andreae, M., Araxo, P., and Maenhaut, W.: Formation of secondary organic aerosols through photooxidation of isoprene, *Science*, 303, 1173–1176, doi:10.1126/science.1092805, 2004.
- Cocker III, D., Flagan, R., and Seinfeld, J.: State-of-the-art chamber facility for studying atmospheric aerosol chemistry, *Environ. Sci. Technol.*, 35, 2594–2601, doi:10.1021/es0019169, 2001.

- Comernolle, S., Ceulemans, K., and Müller, J.-F.: Influence of non-ideality on condensation to aerosol, *Atmos. Chem. Phys.*, 9, 1325–1338, doi:10.5194/acp-9-1325-2009, 2009.
- Edney, E., Kleindienst, T., Jaoui, M., Lewandowski, M., Offenberg, J., Wang, W., and Claeys, M.: Formation of 2-methyltetrols and 2-methylglyceric acid in secondary organic aerosol from laboratory irradiated isoprene/NO_x/SO₂/air mixtures and their detection in ambient PM_{2.5} samples collected in the eastern United States, *Atmos. Environ.*, 39, 5281–5289, doi:10.1016/j.atmosenv.2005.05.031, 2005.
- EPRI: Organic Aerosol Partition Module Documentation, Tech. rep., 1999.
- Ervens, B., Carlton, A., Turpin, B., Altieri, K., Kreidenweis, S., and Feingold, G.: Secondary organic aerosol yields from cloud-processing of isoprene oxidation products, *Geophys. Res. Lett.*, 35, L02816, doi:10.1029/2007GL031828, 2008.
- Fredenslund, A., Jones, R., and Prausnitz, J.: Group-contribution estimation of activity-coefficients in nonideal liquid-mixtures, *AIChE J.*, 21, 1086–1099, 1975.
- Gao, S., Ng, N. L., Keywood, M., Varutbangkul, V., Bahreini, R., Nenes, A., He, J., Yoo, K. Y., Beauchamp, J. L., Hodyss, R. P., Flagan, R. C., and Seinfeld, J. H.: Particle phase acidity and oligomer formation in secondary organic aerosol, *Environ. Sci. Technol.*, 38, 6582–6589, doi:10.1021/es049125k, 2004.
- Goliff, W. and Stockwell, W.: The Regional Atmospheric Chemistry Mechanism, version 2, an update, International Conference on Atmospheric Chemical Mechanisms, University of California, Davis, CA, USA, available at: <http://airquality.ucdavis.edu/pages/events/2008/acm/Goliff.pdf> (last access: August 2010), 2008.
- Guenther, A., Karl, T., Harley, P., Wiedinmyer, C., Palmer, P., and Geron, C.: Estimates of global terrestrial isoprene emissions using MEGAN (Model of Emissions of Gases and Aerosols from Nature), *Atmos. Chem. Phys.*, 6, 3181–3210, doi:10.5194/acp-6-3181-2006, 2006.
- Hilal, S., Ayyampalayam, S., and Carreira, L.: Air-liquid partition coefficient for a diverse set of organic compounds: Henry's law constant in water and hexadecane, *Environ. Sci. Technol.*, 42, 9231–9236, doi:10.1021/es8005783, 2008.
- Jang, M., Czochke, N. M., Lee, S., and Kamens, R.: Heterogeneous atmospheric aerosol production by acid-catalysed particle-phase reactions, *Science*, 298, 814–817, doi:10.1126/science.1075798, 2002.
- Jang, M., Czochke, N. M., and Northcross, A. L.: Semiempirical model for organic aerosol growth by acid-catalyzed heterogeneous reactions of organic carbonyls, *Environ. Sci. Technol.*, 39, 164–174, doi:10.1021/es048977h, 2005.
- Kamens, R., Gery, M., Jeffries, H., Jacksons, M., and Cole, E.: Ozone-isoprene reactions: product formation and aerosol potential, *Int. J. Chem. Kinet.*, 14, 955–975, 1982.
- Kanakidou, M., Seinfeld, J., Pandis, S., Barnes, I., Dentener, F., Facchini, M., Van Dingenen, R., Ervens, B., Nenes, A., Nielsen, C., Swietlicki, E., Putaud, J., Balkanski, Y., Fuzzi, S., Horth, J., Moortgat, G., Winterhalter, R., Myhre, C., Tsigaridis, K., Vignati, E., Stephanou, E., and Wilson, J.: Organic aerosol and global climate modelling: a review, *Atmos. Chem. Phys.*, 5, 1053–1123, doi:10.5194/acp-5-1053-2005, 2005.
- Kim, Y., Sartelet, K., and Seigneur, C.: Comparison of two gas-phase chemical kinetic mechanisms of ozone formation over Europe, *J. Atmos. Chem.*, 62, 89–119, doi:10.1007/s10874-009-9142-5, 2009.
- Kleindienst, T., Lewandowski, M., Offenberg, J., Jaoui, M., and Edney, E.: Ozone-isoprene reactions: Re-examination of the formation of secondary organic aerosol, *Geophys. Res. Lett.*, 34, L01805, doi:10.1029/2006GL027485, 2007.
- Kleindienst, T., Lewandowski, M., Offenberg, J., Jaoui, M., and Edney, E.: The formation of secondary organic aerosols from the isoprene + OH reaction in the absence of NO_x, *Atmos. Chem. Phys.*, 9, 6541–6558, doi:10.5194/acp-9-6541-2009, 2009.
- Kroll, J., Ng, N., Murphy, S., Flagan, R., and Seinfeld, J.: Secondary organic aerosol formation from isoprene photooxidation, *Environ. Sci. Technol.*, 40, 1869–1877, doi:10.1021/es0524301, 2006.
- Kroll, J. H. and Seinfeld, J. H.: Chemistry of secondary organic aerosol: Formation and evolution of low-volatility organics in the atmosphere, *Atmos. Environ.*, 42, 3593–3624, doi:10.1016/j.atmosenv.2008.01.003, 2008.
- Liggio, J., Li, S.-M., and McLaren, R.: Heterogeneous Reactions of Glyoxal on Particulate Matter: Identification of Acetals and Sulfate Esters, *Environ. Sci. Technol.*, 39, 1532–1541, doi:10.1021/es048375y, 2005.
- Meylan, W. and Howard, P.: Bond contribution method for estimating Henry's law constants, *Environ. Toxicol. Chem.*, 10, 1283–1293, doi:10.1002/etc.5620101007, 1991.
- Meylan, W. and Howard, P.: SRC's EPI suite, v3.20, Tech. rep., Syracuse Research Corporation, 2000.
- Ng, N. L., Chhabra, P. S., Chan, A. W. H., Surratt, J. D., Kroll, J. H., Kwan, A. J., McCabe, D. C., Wennberg, P. O., Sorooshian, A., Murphy, S. M., Dalleska, N. F., Flagan, R. C., and Seinfeld, J. H.: Effect of NO_x level on secondary organic aerosol (SOA) formation from the photooxidation of terpenes, *Atmos. Chem. Phys.*, 7, 5159–5174, doi:10.5194/acp-7-5159-2007, 2007a.
- Ng, N. L., Kroll, J. H., Chan, A. W. H., Chhabra, P. S., Flagan, R. C., and Seinfeld, J. H.: Secondary organic aerosol formation from m-xylene, toluene, and benzene, *Atmos. Chem. Phys.*, 7, 3909–3922, doi:10.5194/acp-7-3909-2007, 2007b.
- Ng, N., Kwan, A., Surratt, J., Chan, A., Chhabra, P., Sorooshian, A., Pye, H., Crouse, J., Wennberg, P., Flagan, R., and Seinfeld, J.: Secondary organic aerosol (SOA) formation from reaction of isoprene with nitrate radicals (NO₃), *Atmos. Chem. Phys.*, 8, 4117–4140, doi:10.5194/acp-8-4117-2008, 2008.
- Nguyen, T., Bateman, A., Bones, D., Nizkorodov, S., Laskin, J., and Laskin, A.: High-resolution mass spectrometry analysis of secondary organic aerosol generated by ozonolysis of isoprene, *Atmos. Environ.*, 44, 1032–1042, doi:10.1016/j.atmosenv.2009.12.019, 2010.
- Odum, J., Hoffman, T., Bowman, F., Collins, D., Flagan, R., and Seinfeld, J.: Gas/particle partitioning and secondary organic aerosol yields, *Environ. Sci. Technol.*, 30, 2580–2585, doi:10.1021/es950943+, 1996.
- Pandis, S., Paulson, S., Seinfeld, J., and Flagan, R.: Aerosol formation in the photooxidation of isoprene and β-pinene, *Atmos. Environ.*, 25, 997–1008, doi:10.1021/es0524301, 1991.
- Pankow, J.: An absorption model of gas/particle partitioning of organic compounds in the atmosphere, *Atmos. Environ.*, 28A, 185–188, 1994a.
- Pankow, J.: An absorption model of the gas/aerosol partitioning involved in the formation of secondary organic aerosol, *Atmos.*

- Environ., 28A, 189–193, 1994b.
- Pankow, J. and Asher, W.: SIMPOL.1: a simple group contribution method for predicting vapor pressures and enthalpies of vaporization of multifunctional organic compounds, *Atmos. Chem. Phys.*, 8, 2773–2796, doi:10.5194/acp-8-2773-2008, 2008.
- Pöschl, U., Von Kuhlmann, R., Poisson, N., and Crutzen, P.: Development and intercomparison of condensed isoprene oxidation mechanisms for global atmospheric modeling, *J. Atmos. Chem.*, 37, 29–52, doi:10.1023/A:1006391009798, 2000.
- Pun, B.: Development and initial application of the sesquiverision of MADRID, *J. Geophys. Res.*, 113, D12212, doi:10.1029/2008JD009888, 2008.
- Pun, B. and Seigneur, C.: Investigative modeling of new pathways for secondary organic aerosol formation, *Atmos. Chem. Phys.*, 7, 2199–2216, doi:10.5194/acp-7-2199-2007, 2007.
- Pun, B., Griffin, R., Seigneur, C., and Seinfeld, J.: Secondary organic aerosol 2. Thermodynamic model for gas/particle partitioning of molecular constituents, *J. Geophys. Res.*, 107, 4333, doi:10.1029/2001JD000542, 2002.
- Pun, B., Wu, S.-Y., Seigneur, C., Seinfeld, J., Griffin, R., and Pandis, S.: Uncertainties in Modeling Secondary Organic Aerosols: Three-Dimensional Modeling Studies in Nashville/Western Tennessee, *Environ. Sci. Technol.*, 37, 3647–3661, doi:10.1021/es0341541, 2003.
- Pun, B., Seigneur, C., and Lohman, K.: Modeling secondary organic aerosol formation via multiphase partitioning with molecular data, *Environ. Sci. Technol.*, 40, 4722–4731, doi:10.1021/es0522736, 2006.
- Raventos-Duran, T., Camredon, M., Valorso, R., and Aumont, B.: Structure-activity relationships to estimate the effective Henry's law coefficients of organics of atmospheric interest, *Atmos. Chem. Phys. Discuss.*, 10, 4617–4647, doi:10.5194/acpd-10-4617-2010, 2010.
- Rollins, W., Kiender-Scharr, A., Fry, J., Brauers, T., Brown, S., Dorn, H.-P., Dubé, W., Fuchs, H., Mensah, A., Mentel, T., Tillmann, R., Wegener, R., Wooldridge, P., and Cohen, R.: Isoprene oxidation by nitrate radical: alkyl nitrate and secondary organic aerosol yields, *Atmos. Chem. Phys.*, 9, 6685–6703, doi:10.5194/acp-9-6685-2009, 2009.
- Ruppert, L. and Becker, K.: A product study of the OH radical-initiated oxidation of isoprene: formation of C₅-unsaturated diols, *Atmos. Environ.*, 34, 1529–1542, doi:10.1016/S1352-2310(99)00408-2, 2000.
- Surratt, J., Murphy, S., Kroll, J., Ng, N., Hildebrandt, L., Sorooshian, A., Szmigielski, R., Vermeylen, R., Maenhaut, W., Claeys, M., Flagan, R., and Seinfeld, J.: Chemical composition of secondary organic aerosol formed from the photooxidation of isoprene, *J. Phys. Chem. A*, 110, 9665–9690, doi:10.1021/jp061734m, 2006.
- Surratt, J., Chan, A., Eddingsaas, N., Chan, M., Loza, C., Kwan, A., Hersery, S., Flagan, R., Wennberg, P., and Seinfeld, J.: Reactive intermediates revealed in secondary organic aerosol formation from isoprene, *Proc. Natl. Acad. Sci.*, 107, 6640–6645, doi:10.1073/pnas.0911114107, 2010.
- Suzuki, T., Ohtaguchi, K., and Koide, K.: Application of principal components analysis to calculate Henry's constant from molecular structure, *Computers Chem.*, 16, 41–52, 1992.
- Verwer, J., Spee, E., Bloom, J., and Hundsdoerfer, W.: A second-order rosenbrock method applied to photochemical dispersion problems, *SIAM J. Sci. Comput.*, 20, 1456–1480, doi:10.1137/S1064827597326651, 1999.
- Volkamer, R., Ziemann, P. J., and Molina, M. J.: Secondary Organic Aerosol Formation from Acetylene (C₂H₂): seed effect on SOA yields due to organic photochemistry in the aerosol aqueous phase, *Atmos. Chem. Phys.*, 9, 1907–1928, doi:10.5194/acp-9-1907-2009, 2009.
- Yu, S., Bhave, P., Dennis, R., and Marthur, R.: Seasonal and regional variations of primary and secondary organic aerosols over the Continental United States: Semi-empirical estimates and model evaluation, *Environ. Sci. Technol.*, 41, 4690–4697, doi:10.1021/es061535g, 2007.
- Zhang, Q., Jimenez, J., Canagaratna, M., Allan, J., Coe, H., Ulbrich, I., Alfarra, M., Takami, A., Middlebrook, A., Sun, Y., Dzepina, K., Dunlea, E., Docherty, K., De-Carlo, P., Salcedo, D., Onasch, T., Jayne, J., Miyoshi, T., Shimonono, A., Hatakeyama, S., Takegawa, N., Kondo, Y., Schneider, J., Drewnick, F., Borrmann, S., Weimer, S., Demerjian, K., Williams, P., Bower, K., Bahreini, R., Cottrell, L., Griffin, R., Rautiainen, J., Sun, J., Zhang, Y., and Worsnop, D.: Ubiquity and dominance of oxygenated species in organic aerosols in anthropogenically-influenced Northern Hemisphere midlatitudes, *Geophys. Res. Lett.*, 34, doi:10.1029/2007GL029979, 2007a.
- Zhang, Y., Huang, J.-P., Henze, D., and Seinfeld, J.: Role of isoprene in secondary organic aerosol formation on a regional case, *J. Geophys. Res.*, 112, D20 207, doi:10.1029/2007JD008675, 2007b.
- Zuend, A., Marcolli, C., Peter, T., and Seinfeld, J. H.: Computation of liquid-liquid equilibria and phase stabilities: implications for RH-dependent gas/particle partitioning of organic-inorganic aerosols, *Atmos. Chem. Phys.*, 10, 7795–7820, doi:10.5194/acpd-10-12497-2010, 2010.